Energy Proceedings
Vol 49, 2024
ISSN 2004-2965

Temperature-jump during Ethanol Evaporation in Cylindrical Pool Heated from Bottom at Low Pressure[#]

Chuan-Long Ge, Hua-Yang Liu, You-Rong Li[*]

College of energy and power engineering, Chongqing University

(*Corresponding Author: liyourong@cqu.edu.cn)

ABSTRACT

In this paper, a series of evaporation experiments were carried out on a cylindrical pool. From these experimental results, we obtain the axial temperature distribution of the ethanol evaporation process, and compare the results of different heating temperatures at different depths. The results indicate that the evaporation of ethanol with different depths will bring different flow patterns, thus changing the temperature distribution. At the same time, we also determined the temperature jump range of ethanol evaporation in cylindrical pool heated from the bottom.

Keywords: evaporation, cylindrical pool, temperature-jump.

1. INTRODUCTION

Evaporation process widely exists in nature and engineering technology. It is a typical non-equilibrium thermodynamic process. At present, evaporation process widely exists in perovskite solar cell processing[1], modern agricultural technology[2], inkjet printing[3], electronic testing[4], solar steam generator[5] and other technical fields, and has an important impact on the quality of finished products in the above process. Therefore, it is necessary to have a further study on the evaporation process.

At present, there are three main theories about evaporation process: Hertz−Knudsen theory [i.e., kinetic theory of gases (KTG)[6]], statistical rate theory (SRT)[7,8], and non-equilibrium thermodynamics (NET)[9]. In the KTG model, evaporation occurs in the vapor layer with several molecular average free path thicknesses near the gas-liquid interface. This vapor layer is called the Knudsen layer, During the evaporation process, molecules will enter the liquid phase from the vapor phase, and molecules will also enter the gas phase from the liquid phase.

In the evaporation process, according to the KTG theory mentioned above, the discontinuity process is assumed to occur only in the Knudsen layer. At this time, the temperature on both sides of the Knudsen layer can be regarded as the vapor temperature and the liquid temperature near the vapor-liquid interface. At this time, the temperature difference between the two temperatures is the temperature jump of the vapor-liquid interface. Many studies[10–13] have confirmed the existence of temperature discontinuity at the vapor-liquid interface by direct measurement using micro-thermocouples. The results of kinetic theory model[14], Monte Carlo simulation[15] and molecular dynamics simulation[16] have confirmed that the existence of temperature jump.

Among the temperature-jump measured by the evaporation experiment at low-pressure, the temperature of vapor side is higher than the liquid side. However, when evaporating in an open environment at atmospheric phenomenon, the relative temperature of the two-phase side of the interface is reversed, This is also verified in some studies[11,17].

In summary, there are a large number of experimental and theoretical studies. However, the temperature jump of ethanol evaporation process at low pressure and the range of temperature jump have not been determined. Here, we have conducted a series of evaporation experiments on the liquid-vapor interfacial in a cylindrical pool. Through the micro thermocouple, we can get the temperature distribution of the vapor and liquid phase, and determine the value of the temperature jump.

2. EXPERIMENTAL INVESTIGATION

2.1 Experimental Setup

The experimental components is shown in Fig. 1. The whole experimental system is mainly composed of

[#] This is a paper for the 16th International Conference on Applied Energy (ICAE2024), Sep. 1-5, 2024, Niigata, Japan.

sealing evaporation cavity, liquid injection system, temperature control and measurement system, pressure control and measurement system and data acquisition system. The cylindrical pool is made by red copper. The cylindrical pool is placed at the bottom of a closed sealing evaporation cavity with a wall thickness of 10 mm. The low pressure environment is maintained by a rotary vane vacuum pump, and the vapor pressure can be precisely controlled by a metering valve and monitored in real time through a pressure transducer (CDG025D, INFICON). The sensor is 100 mm away from the vapor-liquid interface. The inner diameter and depth of the cylindrical pool are 80 mm and 35 mm. The temperature measurement position is 10 mm away from the center line of the cylindrical pool. Figs. 2 is the three-dimensional model diagram.

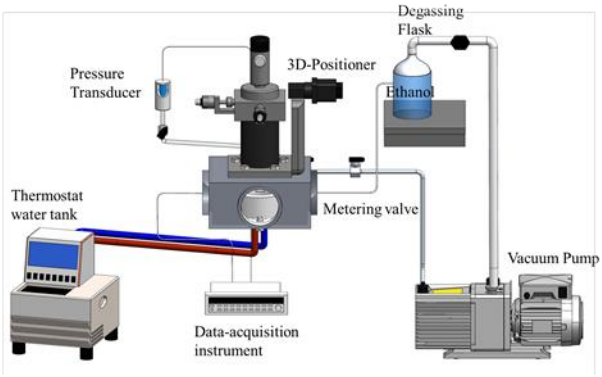

Fig. 1 Schematic of the experimental system

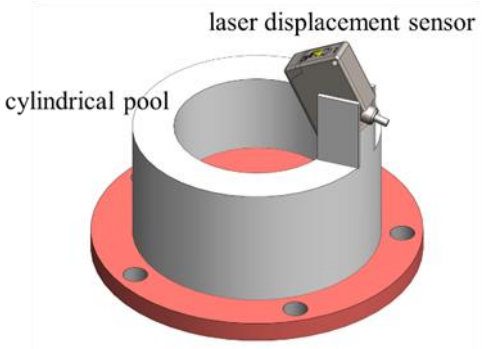

Fig. 2 The cylindrical pool and the laser displacement sensor

Eight T-type thermocouples with a diameter of 127 μm embedded in the bottom to measure the bottom temperature. The liquid layer depth is determined by a laser displacement sensor (OPTEX CD33) fixed on the outer wall of the cylindrical pool. Because of no supplement of liquid during temperature measurement, the average evaporation rate of the whole interface during the temperature measurement can be obtained by calculating variation rate of liquid layer depth with measuring time for the measurement of temperature. A T-type thermocouple with a diameter of 50 μm is fixed on a three-dimensional (3D) positioner Therefore, the liquid and vapor phase temperatures can be measured by controlling 3D positioner. The accuracy of 3D positioner is 1 μm in *z* direction Under experimental conditions, the depth (*d*) of ethanol ranges from 5 to 15 mm The temperatures of heating temperature ranges from 1 °C to 10 °C. For convenience to evaluate the relative vapor pressure at different experimental conditions, the pressure ratio (β) is introduced in this work, which is described by.

$$\beta = \frac{P^V}{P_{sat}(T_W)} \tag{1}$$

2.2 Experimental Procedures

Before the experiment, the ethanol in the degassing bottle is allowed to enter the injection pump without contact with the air. At the same time, the vacuum pump continues to exhaust the cavity. Next, the constant temperature water bath temperature will be adjusted according to the set working conditions to maintain the heating wall temperature unchanged. The injection pump pumps ethanol into the liquid pool, and the initial depth should be 2-3 mm higher than the depth to be measured. The depth of the working medium is measured in real time by a laser displacement sensor. The vapor pressure in the cavity is controlled by adjusting the precise control valve connected to the vacuum pump. When the vapor pressure is maintained at the predetermined pressure of the experiment for 60 min, it can be considered that the chamber reaches a stable-evaporation condition. When the depth of ethanol in the pool drops to the depth to be measured, At this time, the temperature can be measured by moving the thermocouple. the axial temperature distribution at the radial position can be obtained, and the temperature-jump can be determined.

3. RESULTS AND ANALYSIS

A series of steady-state evaporation experiments were conducted on ethanol under different pressure, different depths and temperature conditions. In the first set of experiments, we set up the heating temperature was 10 °C. Then we get the temperature profile at different pressures and different depths at this heating temperature. In all sets of experiments, the vapor pressure of the system and the depths of the system was varied to study the influence of vapor pressure and depths on evaporation. The temperature profiles in the liquid and vapor phases in all of these experiments are

shown in Figures 3, 4 and 5. Pools of different depths have different internal flow, so the axial temperature distribution is also different. Note that the range of pressure at different depths is different, because the critical pressure ratio of instability at different depths is different.

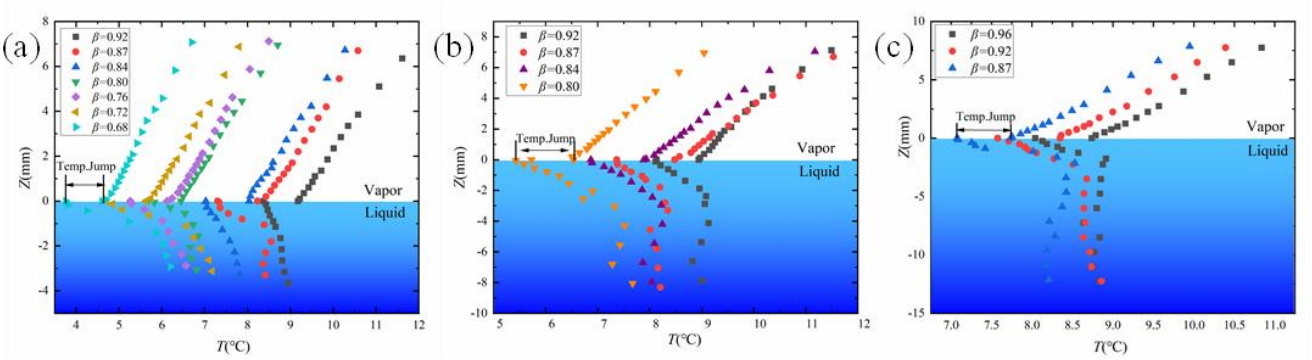

Fig. 3 Temperature profile along the vertical axis at different vapor pressure rates when T_w = 10 °C, d = 5 mm (a), d = 10 mm (b) and d=15 mm(c).

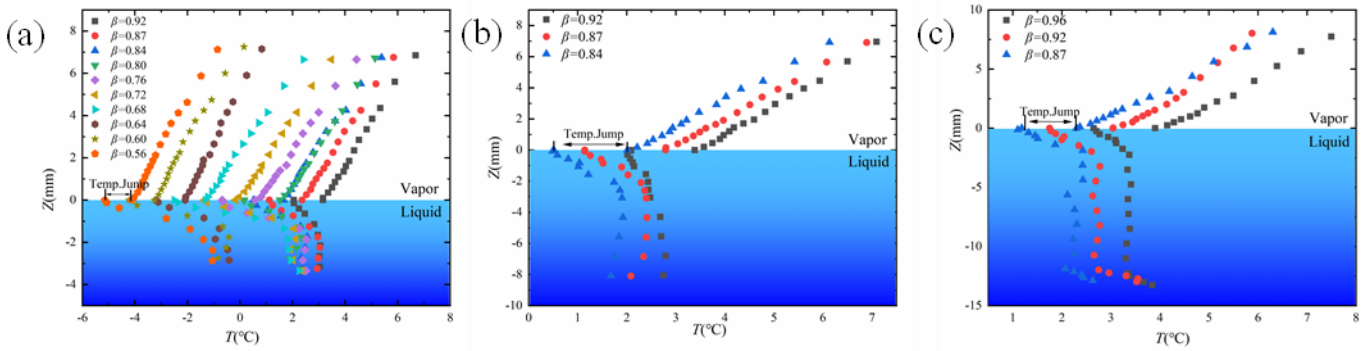

Fig. 4 Temperature profile along the vertical axis at different vapor pressure rates when T_w = 4 °C, d = 5 mm (a), d = 10 mm (b) and d=15 mm(c).

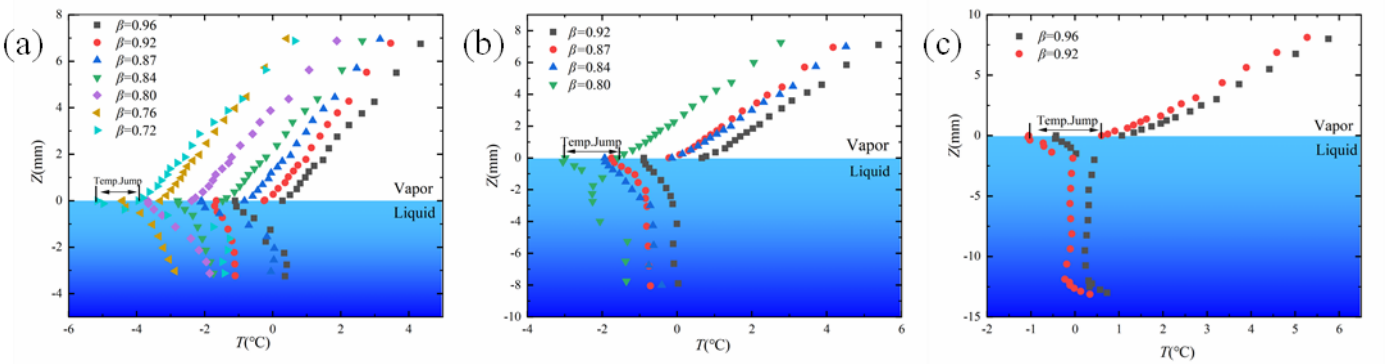

Fig. 5 Temperature profile along the vertical axis at different vapor pressure rates when T_w = 1 °C, d = 5 mm (a), d = 10 mm (b) and d=15 mm(c).

In all experiments, there is a temperature discontinuity (temperature jump) at the liquid-vapor interface, and the temperature in the vapor phase is slightly higher than that in the liquid phase. The results show that due to the evaporative cooling effect, the lowest temperature at all experiments appears at the liquid-vapor interface. In the vicinity of the interface, the temperature distribution is linear, which indicates that heat conduction is the main way of energy transfer to the interface. The heat fluxes on the liquid and vapor sides are calculated from the temperature profiles. In all experiments, the range of temperature jump is about 0.9 °C -1.9 °C.

4. CONCLUSIONS

A series of evaporation experiments were carried out on a cylindrical pool. In all of the experiments, the

interfacial vapor temperature was higher than that of the liquid. According to the experimental results, the temperature jump and evaporation rate under different experimental conditions were obtained. In all experiments, the range of temperature jump is about 0.9 ℃ -1.9 ℃. Pools of different depths have different internal flow, so the axial temperature distribution is also different.

ACKNOWLEDGEMENT

This work is supported by the National Natural Science Foundation of China (Grant No.52076017)

REFERENCE

[1] Ahmadian-Yazdi M-R, Barratt C, Rahimzadeh A, et al. Microstructural and nanostructural evolution of light harvester perovskite thin film under the influence of ultrasonic vibrations. ACS Omega, 2020, 5(1): 808–821.

[2] Liu H, Duan A, Li F, et al. Drip irrigation scheduling for tomato grown in solar greenhouse based on pan evaporation in north China plain. Journal of Integrative Agriculture, 2013, 12(3): 520–531.

[3] Talbot EL, Yang L, Berson A, et al. Control of the particle distribution in inkjet printing through an evaporation-driven sol–gel transition. ACS Applied Materials & Interfaces, 2014, 6(12): 9572–9583.

[4] Ahmadian-Yazdi M-R, Eslamian M. Effect of Marangoni convection on the perovskite thin liquid film deposition. Langmuir, 2021, 37(8): 2596–2606.

[5] Zhao C, Tan C, Lien D-H, et al. Evaporated tellurium thin films for p-type field-effect transistors and circuits. Nature Nanotechnology, 2020, 15(1): 53–58.

[6] Knudsen M. Maximum rate of vaporisation of mercury. Annals of Physics, 1915, 352(13): 697–708.

[7] Ward CA, Findlay RD, Rizk M. Statistical rate theory of interfacial transport. I. Theoretical development. The Journal of Chemical Physics, 1982, 76(11): 5599–5605.

[8] Ward CA, Rizk M, Tucker AS. Statistical rate theory of interfacial transport. II. Rate of isothermal bubble evolution in a liquid–gas solution. The Journal of Chemical Physics, 1982, 76(11): 5606–5614.

[9] Badam VK, Kumar V, Durst F, et al. Experimental and theoretical investigations on interfacial temperature jumps during evaporation. Experimental Thermal and Fluid Science, 2007, 32(1): 276–292.

[10] Shankar PN, Deshpande MD. On the temperature distribution in liquid–vapor phase change between plane liquid surfaces. Physics of Fluids A: Fluid Dynamics, 1990, 2(6): 1030–1038.

[11] Zhu Z-Q, Liu Q-S. Interfacial temperature discontinuities in a thin liquid layer during evaporation. Microgravity Science and Technology, 2013, 25(4): 243–249.

[12] Gatapova EYa, Filipenko RA, Lyulin YuV, et al. Experimental investigation of the temperature field in the gas-liquid two-layer system. Thermophysics and Aeromechanics, 2015, 22(6): 701–706.

[13] Fang G, Ward CA. Temperature measured close to the interface of an evaporating liquid. Physical Review E, 1999, 59(1): 417–428.

[14] Aoki K, Masukawa N. Gas flows caused by evaporation and condensation on two parallel condensed phases and the negative temperature gradient: Numerical analysis by using a nonlinear kinetic equation. Physics of Fluids, 1994, 6(3): 1379–1395.

[15] Jafari P, Amritkar A, Ghasemi H. Temperature discontinuity at an evaporating water interface. The Journal of Physical Chemistry C, 2020, 124(2): 1554–1559.

[16] Liang Z, Evans W, Keblinski P. Equilibrium and nonequilibrium molecular dynamics simulations of thermal conductance at solid-gas interfaces. Physical Review E, 2013, 87(2): 022119.

[17] Gatapova EYa, Graur IA, Kabov OA, et al. The temperature jump at water – air interface during evaporation. International Journal of Heat and Mass Transfer, 2017, 104: 800–812.